Comparative structural studies of Ni *vs*. Au metal bis-dithiolene complexes with a thiazole backbone [M(R-thiazdt)$_2$]

Dr. Agathe Filatre-Furcate, Dr. Thierry Roisnel, Yann Le Gal, Dr. Olivier Jeannin, Dr. Vincent Dorcet, and Prof. Dr. Dominique Lorcy*

Univ Rennes, CNRS, ISCR (Institut des Sciences Chimiques de Rennes) - UMR 6226, F-35000 Rennes, France. E-mail: Dominique.lorcy@univ-rennes1.fr.

Abstract

Monoanionic nickel bis(dithiolene) complexes formulated as [Ni(R-thiazdt)$_2$]$^{-1}$ with R = Pr, cPr, NMe$_2$ and *i*Pr were prepared in order to analyze the influence of bulky substituents on the organization of these electroactive molecules in the solid state. Electrochemical and spectroelectrochemical investigations shed lights on the redox and optical properties of the monoanionic and neutral states of these complexes. The crystal structure of the monoanionic and neutral species [Ni(R-thiazdt)$_2$]$^{-1,0}$ with R = NMe$_2$ and *i*Pr shows that despite similar steric hindrance of the substituents, the solid state organization is different. Comparison of the neutral structures of the two structurally characterized neutral nickel complexes with their gold analogues demonstrates the role played on the organization by the nature of the metal, leading to closed-shell *vs* open-shell complexes.

Introduction

In the two last decades, nickel and gold bis(dithiolene) complexes have received a special attention as precursors of single component molecular conductors[1-3] especially after the discovery of highly conducting complexes involving two TTF-dithiolate ligands around the metal center. [4-5] This active research topic is motivated by the advantages that single-component materials can bring, compared to multi-component materials (ion radical salts, charge transfer salts) where one of the component, the counterion, rather plays a spectator role. Thus, the lack of counterion can increase the intermolecular interactions between the

electroactive components and generate highly conducting materials.[1-5] These neutral complexes, despite their neutral structure, present some differences as the neutral gold bis(dithiolene) complexes are *open-shell* species while the neutral nickel complexes are *closed-shell* species. Another interesting point is their organization in the solid state. Among the different neutral nickel and gold bis(dithiolene) complexes described to date, with the same ligand, isostructural pairs are found generally in the complexes with bulky dithiolene ligands where the bulky substituents usually hindered a close packing of the molecules.[6-12] On the other hand, for less-hindered ligands, the Ni and Au complexes are not isostructural,[12-21] except if non-covalent interactions favor specific intermolecular interactions between neighbouring complexes such as hydrogen bonding in [M(HOEtS-tzdt)$_2$] (M = Au,Ni) where isostructural complexes were obtained.[22] These different organizations in non-hindered complexes are correlated with the radical nature of the gold dithiolene complexes, where stabilization through overlap interaction favors short intermolecular contacts between the central parts, [Au(S_2C_2)$_2$] metallacycles, of the complexes. The organization of the corresponding nickel complexes, lacking this extra electron, is controlled exclusively by non-bonding intermolecular interactions. We are currently investigating complexes derived from N-alkyl-1,3-thiazoline-2-thione-4,5-dithiolate (R-thiazdt), either the gold [Au(R-thiazdt)$_2$]$^{\bullet}$ or the nickel [Ni(R-thiazdt)$_2$]^0 as precursor of single component molecular conductors. In this series, only the ethyl and methyl substituted neutral nickel complexes [Ni(R-thiazdt)$_2$] (R = Et, Me)[19] were characterized so far and their organization in the solid state differs from the one of the corresponding neutral gold complexes [Au(R-thiazdt)$_2$] (R = Et, Me)[20] Among the different gold complexes with the R-thiazdt ligand, we investigated the complexes substituted with bulkier R groups such as propyl, isopropyl, dimethyl amino and cyclopropyl groups, [Au(R-thiazdt)$_2$] (R = Pr, *i*Pr, NMe_2, *c*Pr) (Scheme 1).[23,24] Thus we decided to analyze the corresponding neutral nickel complexes, with the same bulkier substituents i.e. [Ni(R-thiazdt)$_2$]

(R = Pr, *i*Pr, NMe_2, *c*Pr), in order to see the impact of these bulky substituents on the organization of the complexes in the solid state (Scheme 1). Here in we present the synthesis of these four nickel complexes together with the crystal structures investigations of the radical anion and the neutral complexes $[Ni(R\text{-}thiazdt)_2]^{-1,0}$ with R = *i*Pr and NMe_2. Comparative study with their gold analogues will be also investigated.

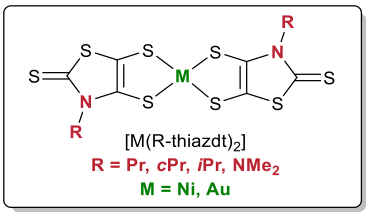

Scheme 1. Target metal bis(dithiolene) complexes

Results and Discussion

The synthesis of the neutral Ni complexes, $[Ni(R\text{-}thiazdt)_2]$ (R = Pr, *i*Pr, NMe_2, *c*Pr), starting from the proligands **1-R**[23,24] was performed as depicted in Scheme 2. First, the Ni complexes were prepared under the dianionic state, $[PPh_4]_2[Ni(R\text{-}thiazdt)_2]$, by deprotecting the thiolate functions of **1-R** in the presence of sodium methanolate followed by the addition of $NiCl_2$ and PPh_4Cl (Scheme 2). Recrystallization of these dianionic complexes in acetonitrile in air afforded the anion radical species, $[PPh_4][Ni(R\text{-}thiazdt)_2]$. Another possibility to generate the monoanionic complex from the dianionic ones consist in adding one equivalent of $[Cp_2Fe][PF_6]$ to a dichloromethane solution of $[PPh_4]_2[Ni(R\text{-}thiazdt)_2]$ under inert atmosphere. The monoanionic $[PPh_4][Ni(R\text{-}thiazSdt)_2]$ (R = Pr, *c*PR, *i*Pr, NMe_2) complexes were isolated as red crystals after recrystallization in CH_3CN/toluene (1/1). To generate the neutral species, electrocrystallization was performed using the monoanionic complex as starting material. Accordingly, the neutral complexes $[Ni(R\text{-}thiazSdt)_2]^0$ (R = *i*Pr, NMe_2) were isolated as tiny thin black crystals at the anode.

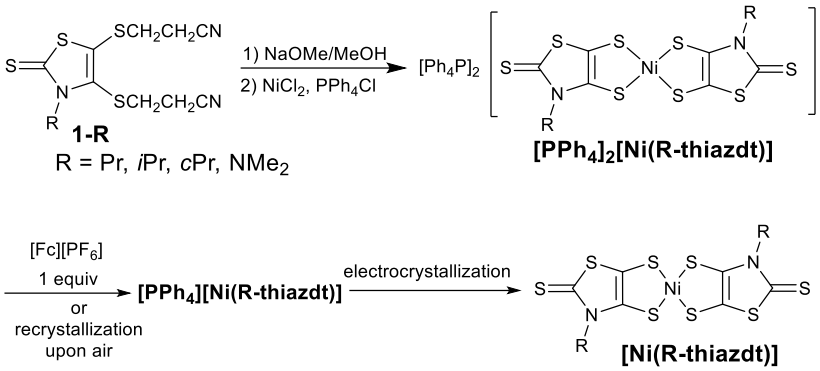

Scheme 2. Synthetic path to the neutral Ni complexes [Ni(R-thiazdt)$_2$]

Electrochemical properties. The redox properties of the Ni complexes were investigated starting from the monoanionic species, [PPh$_4$][Ni(R-thiazdt)$_2$] (R = Pr, *i*Pr, *c*Pr, NMe$_2$), by cyclic voltammetry experiments performed in CH_2Cl_2 using [NBu$_4$][PF$_6$] as supporting electrolyte. Redox potentials, given in V *vs*. SCE, are collected in Table 1 together with the complexes, previously investigated [PPh$_4$][Ni(R-thiazdt)$_2$] (R = Et, Me).[19] For all the investigated complexes three redox processes can be observed on the cyclic voltammogram. Upon anodic scan, the mononanion radical is reversibly oxidized to the neutral species at E^2(–1/0) and then to the monocationic complex at E_{pa}^3. The later process is not fully reversible as can be seen in Figure 1. Then upon cathodic scan, the monoanion radical is reversibly reduced to the dianionic species at E^1(–2/–1). As expected, changing the alkyl substituent on the nitrogen atom of the thiazoline ring does not modify significantly the redox potentials of the different complexes studied (Table 1).

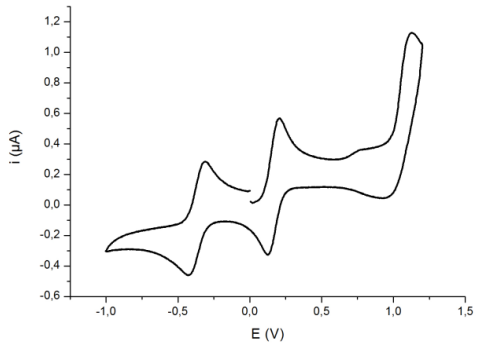

Figure 1. Cyclic voltammogram of $[PPh_4][Ni(Pr\text{-}thiazdt)_2]$ in CH_2Cl_2 with $[NBu_4][PF_6]$ 0.1 M as electrolyte, E in V *vs.* SCE, scan rate 100 $mV.s^{-1}$.

Table 1 Redox potentials in CH_2Cl_2 with $[NBu_4][PF_6]$ 0.1 M, E in V *vs* SCE, scan rate 100 $mV.s^{-1}$, absorption maxima λ_{max} (nm) and molar exctinction coefficients for the NIR absorptions of the investigated Ni complexes.

				λmax(ε)(nm, $M^{-1}cm^{-1}$).	
	E^1	**E^2**	**E_{pa}[3]**	**Anion radical**	**Neutral**
$[Ni(Me\text{-}thiazdt)_2]$[19]	–0.33	+0.18/-0.01[a]	–	1278(20880)	1012
$[Ni(Et\text{-}thiazdt)_2]$[19]	–0.37	+0.17	+1.12*	1280(21000)	1022
$[Ni(Pr\text{-}thiazdt)_2]$	–0.36	+0.17	+1.13*	1282(17690)	1026
$[Ni(i\text{Pr-}thiazdt)_2]$	–0.36	+0.17	+1.00*	1290(17400)	1018
$[Ni(c\text{Pr-}thiazdt)_2]$	–0.38	+0.20/-0.05[a]	+1.15*	1250(17700)	1016
$[Ni(NMe_2\text{-}thiazdt)_2]$	–0.39	+0.135	+1.08*	1242(20810)	1002

*Not fully reversible process. [a] E_{pa}/E_{pc} , E_{pa} and E_{pc} : anodic and cathodic peak potentials. $E = (E_{pa} + E_{pc})/2$

UV-vis-NIR spectroelectrochemical properties. The absorption properties of the monoanionic species were first measured in CH_2Cl_2 at room temperature. They all exhibit a strong electronic absorption in the NIR region at 1242-1290 nm. UV-vis-NIR spectroelectrochemical investigations were carried out on a dichloromethane solution of the monoanionic species in CH_2Cl_2-$[NBu_4][PF_6]$ 0.2 M solution (Figure 2). These investigations give access to the absorption signature of the neutral species but due to partial adsorption of the neutral species onto the electrode it was not possible to determine the absorption coefficient for these neutral species. The gradual oxidation of the monoanionic complexes to the neutral species induces the

decrease of the lowest energy absorption band at the expense of the growth of novel band at higher energy which emerges on the spectra at 1002-1026 nm characteristic of the neutral complexes. This confirms that regardless of the degree of oxidation of the nickel complex, the alkyl group within this study has very little influence on the optical properties of the bis(1,2-dithiolene) nickel complexes.

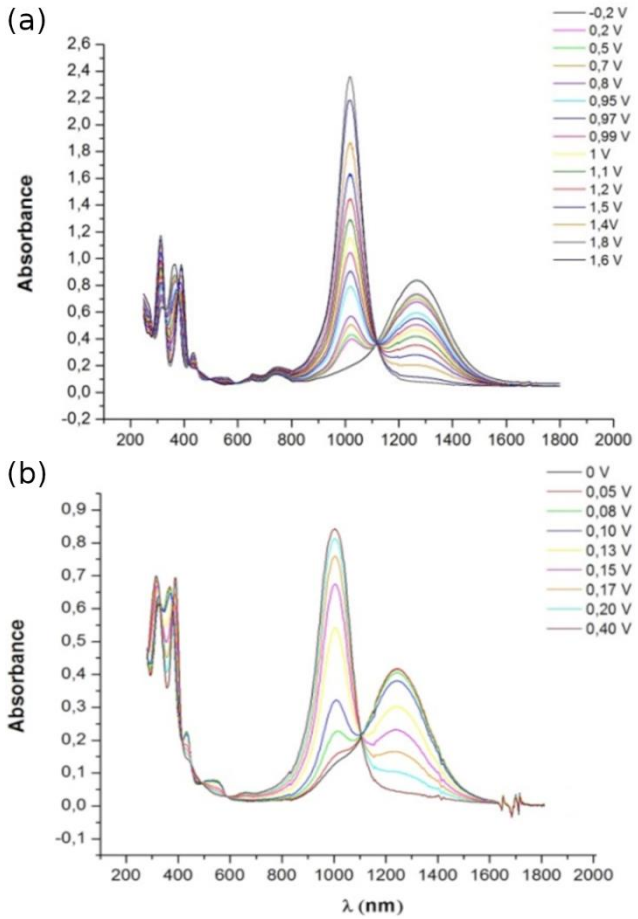

Figure 2. UV-vis-NIR monitoring of the electrochemical oxidation of monoanionic complexes, (a) $[PPh_4][Ni(i\text{Pr-thiazdt})_2]$ (c = 4.7 10^{-4} M) and (b) $[PPh_4][Ni(NMe_2\text{-thiazdt})_2]$ (c = 2 10^{-4} M) into the neutral species. Experiment performed in CH_2Cl_2 with $[NBu_4][PF_6]$ 0.2 M as electrolyte.

Comparative study of the molecular structures of the $[Ni(R\text{-thiazdt})_2]^{-1,0}$ complexes (R = cPr, iPr, NMe_2). The monoanionic complexes crystallize as Ph_4P^+ salt in the monoclinic system,

space group C2/c for $[PPh_4][Ni(R\text{-}thiazdt)_2]$ (R = *c*Pr and *i*Pr) and space group $P2_1/n$ for $[PPh_4][Ni(NMe_2\text{-}thiazdt)_2]$. These salts are isostructural with their monoanionic gold complexes analogues, $[Ph_4P][Au(R\text{-}thiazdt)_2]$ (R = *i*Pr,[23] NMe_2[24]) while the gold complex with a cyclopropyl group was only prepared as a Et_4N^+ salt, $[Et_4N][Au(c\text{Pr-}thiazdt)_2]$. The molecular structure of the anion radical species are depicted in Figure 3 and selected bond lengths and angles are collected in Table 2. An interesting feature with these complexes is that they are all characterized by a *trans* configuration of the dithiolene ligands, with a square planar geometry around the nickel atom. Indeed, due to the dissymmetry of the dithiolene ligand, these complexes are susceptible to exist under two configurations, the *trans* and *cis* isomers, which are easily interconverted at room temperature.[25] However, as previously reported for analogous Ni complexes with Me-thiazdt ligands, it is not possible to detect the *cis* and *trans* isomers by spectroscopic methods.[26] For $[Ni(c\text{Pr-}thiazdt)_2]^{-1}$, the cyclopropyl groups are located above and below the complex skeleton as previously observed for the gold analogue, $[Au(c\text{Pr-}thiazdt)_2]$[24] On the other hand, for $[Ni(R\text{-}thiazdt)_2]^{-1}$ R = *i*Pr and NMe_2 the non-cyclic structure of these groups allows for a different disposition where one methyl group is located above and the other methyl below the plane of the complex. Moreover, the two C–H of the isopropyl groups are pointing towards the metallacycles for $[Ni(iPr\text{-}thiazdt)_2]^{-1}$ and the two lone pairs of the NMe_2 groups oriented towards the metallacycles for $[Ni(NMe_2\text{-}thiazdt)_2]^{-1}$ leading to a *syn*/*syn* conformation of the *i*Pr and NMe_2 groups. This *syn/syn* orientation of the *i*Pr and NMe_2 groups recalls the one observed for the gold complexes analogues.[23,24] The metallacycles are slightly distorted along the S•••S axis with angles from 2.4 to 4.7° (Table 2).

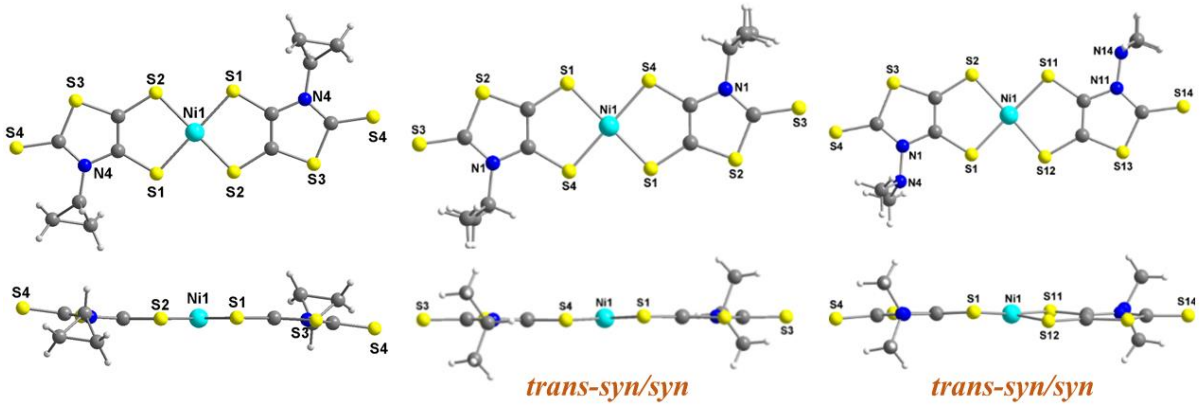

Figure 3. Molecular view of the anion radical species : [Ni(*c*Pr-thazdt)$_2$]$^{-1}$ (left), [Ni(*i*Pr-thazdt)$_2$]$^{-1}$ (middle) and [Ni(NMe$_2$-thiazdt)$_2$]$^{-1}$ (right).

Concerning the neutral complexes, [Ni(*i*Pr-thiazdt)$_2$] crystallizes in the monoclinic system, space group C2/c and [Ni(NMe$_2$-thiazdt)$_2$] crystallizes in the monoclinic system, space group P2$_1$/c. These neutral nickel complexes are not isostructural anymore with their neutral gold complexes analogues. As shown in Figure 4, the [Ni(*i*Pr-thiazdt)$_2$] complex adopts a *cis* configuration, while the [Ni(NMe$_2$-thiazdt)$_2$] complex adopts a *trans* configuration. The *cis* configuration is rather unusual in nickel bis(dithiolene) complexes but results essentially from the solid state organization. It should be noted that several electrocrystallization experiments were performed leading each time to the same structure. The disposition of the NMe$_2$ groups on the [Ni(NMe$_2$-thiazdt)$_2$] complex is the same as that observed for the monoanionic species which is a *syn/syn* conformation with the lone pairs of the nitrogen atoms oriented towards the metallacycles. This *syn*/*syn* conformation of the NMe$_2$ was also observed in the two redox states of the gold complexes [Au(NMe$_2$-thiazdt)$_2$]$^{-1,0}$. A plausible explanation would be that this orientation of the NMe$_2$ would be due to favorable stabilizing electrostatic interactions between the electronic density on the nitrogen atom with the charge depletion on the sulfur atom of the metallacycle. Contrariwise, the orientation of the *i*Pr groups in the neutral complex, [Ni(*i*Pr-thiazdt)$_2$], is different that the one observed for the monoanionic species. This time the hydrogen atoms are oriented towards the C=S leading to an *anti/anti* conformation. The same *anti/anti*

conformation was found on the neutral gold complex, [Au(*i*Pr-thiazdt)$_2$].[23] Thus, in both metal complexes, Ni vs Au, the *syn*/*syn* conformation was found in the monoanionic species, R = *i*Pr and NMe_2 and in the neutral NMe_2 complexes while the *anti*/*anti* conformation was observed in the neutral *i*Pr complexes.

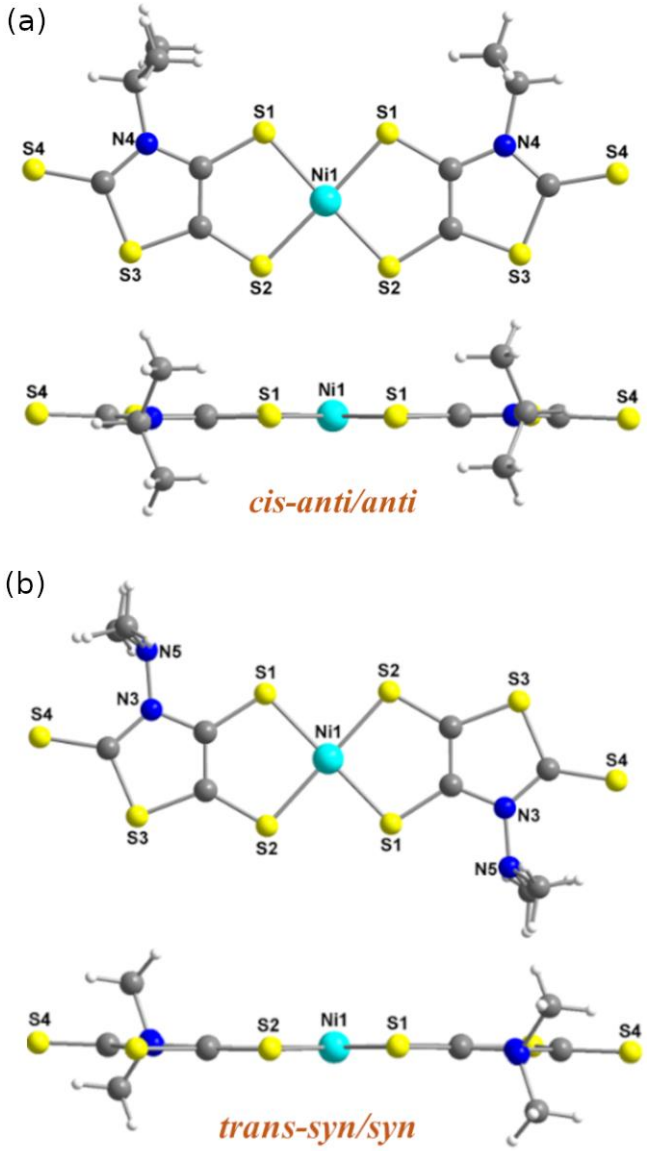

Figure 4. Molecular view and side view of the neutral complexes [Ni(*i*Pr-thazdt)$_2$] (a) and [Ni(NMe_2-thiazdt)$_2$] (b).

Comparison of the bond length between the monoanionic and the neutral species of [Ni(*i*Pr-thiazdt)$_2$]$^{-1,0}$ and [Ni(NMe_2-thiazdt)$_2$]$^{-1,0}$ shows that oxidation induces some modifications on

the intramolecular bond distances essentially on the metallacycle, with the shortening of the C–S bonds and lengthening of the C=C bond (Table 2). Such evolution of the geometrical characteristics upon oxidation of Ni bis(dithiolene) complexes is regularly observed and is the signature of the non-innocent character of the dithiolene ligand.[27] A planarization of the metallacycles of the two neutral complexes is also observed with very small S•••S folding angles of 1.42-1.93° compared with the monoanionic species

Table 2. Intramolecular bond lengths (in Å) in monoanionic and neutral dithiolene complexes $[Ni(i\text{Pr-thiazdt})_2]^{-1,0}$ and $[Ni(NMe_2\text{-thiazdt})_2]^{-1,0}$, together with the folding angle $\theta_{S\cdots S}$ (in °) of the metallacycle along the S•••S axis.

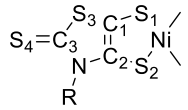	Radical anion		Neutral	
	R = *i*Pr	**R = NMe$_2$**	**R = *i*Pr**	**R = NMe$_2$**
Ni-S_1	2.160(1)	2.1762(8) 2.1710(8)	2.1508(4)	2.1532(4)
Ni-S_2	2.181(1)	2.1688(8) 2.1815(8)	2.1495(4)	2.1572(4)
C_1-S_1	1.715(5)	1.717(3) 1.708(3)	1.693(1)	1.690(2)
C_2-S_2	1.728(3)	1.715(3) 1.722(3)	1.699(1)	1.691(2)
C_1-C_2	1.366(5)	1.358(4) 1.362(4)	1.394(2)	1.381(2)
C_1-S_3	1.742(3)	1.757(3) 1.744(3)	1.732(1)	1.742(2)
S_3-C_3	1.738(5)	1.756(3) 1.755(3)	1.745(1)	1.757(2)
C_3-N	1.372(5)	1.361(4) 1.373(4)	1.374(2)	1.376(2)
C_2-N	1.403(6)	1.402(4) 1.404(4)	1.386(2)	1.385(2)
S_4-C_3	1.671(5)	1.660(3) 1.657(3)	1.651(1)	1.642(2)
$\theta_{S\cdots S}$ (°)	3.13(7)	4.68(6) 2.42(6)	1.42(3)	1.94(3)

Organization of the monoanionic complexes in the solid state. In the solid state the monoanionic complexes, [Ph_4P][Ni(*c*Pr-thiazdt)$_2$] and [Ph_4P][Ni(*i*Pr-thiazdt)$_2$] are isolated from each other in the *ac* plane by the PPh_4^+ couterion (Figure 5a and 5b). Several S•••S contacts in the 3.5-3.6 Å range, between the [Ni(*i*Pr-thiazdt)$_2$]$^{-1}$ and [Ni(*i*Pr-thiazdt)$_2$]$^{-1}$ complexes can be noticed along the *b* axis. This organization is reminiscent to the one observed for the N-Et analogue, [Ph_4P][Ni(Et-thiazdt)$_2$].[19]

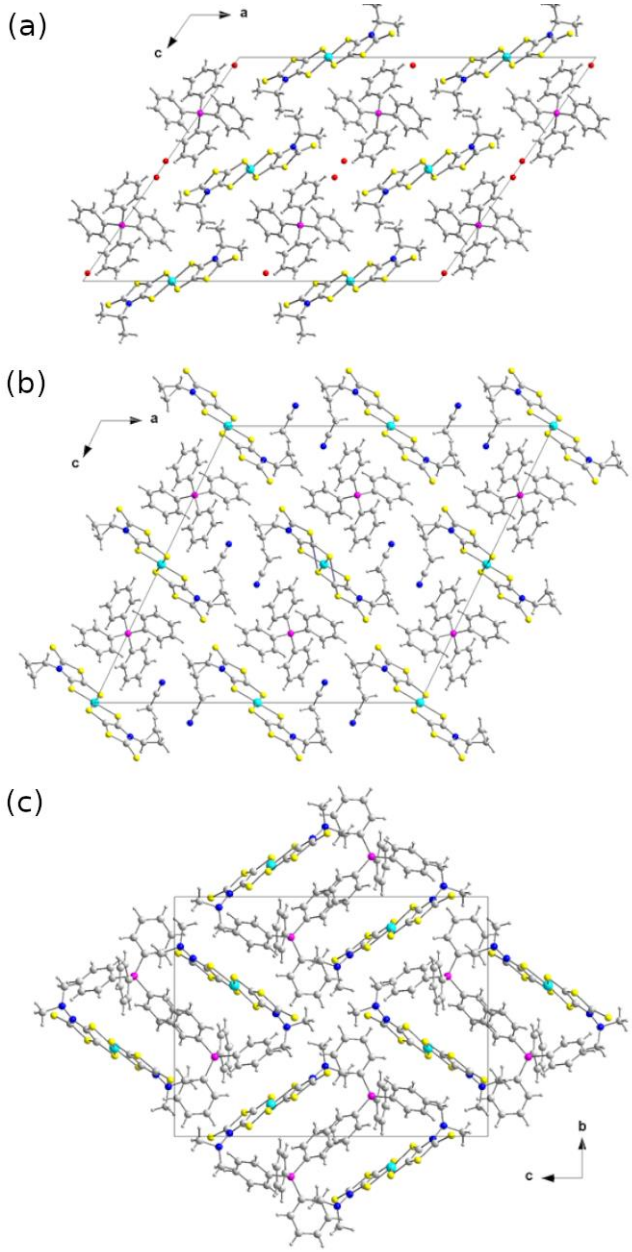

Figure 5. Projection view along the *b* axis of the unit cell of (a) [Ph_4P][Ni(*i*Pr-thiazdt)$_2$] and (b) [Ph_4P][Ni(*c*Pr-thiazdt)$_2$]. (c) Projection view along the *a* axis of the unit cell of [Ph_4P][Ni(NMe_2-thiazdt)$_2$].

Concerning the organization of the $[Ph_4P][Ni(NMe_2\text{-thiazdt})_2]$ complexes in the solid state, the monoanionic complexes, $[Ni(NMe_2\text{-thiazdt})_2]^{-1}$ are there again isolated from each other in the *bc* plane by the PPh_4^+ counterion (Figure 5c). No S•••S contacts shorter than the sum of the van der Waals radii of sulfur could be detected in this organization between the monoanionic species, $[Ni(NMe_2\text{-thiazdt})_2]^{-1}$. The monoanionic nickel complexes are paramagnetic with S = ½, thus we investigated the temperature dependence of the magnetic susceptibility of polycrystalline samples of the complexes where S•••S contacts shorter than the sum of the van der Waals radius of sulfur were detected, which is to say for $[Ph_4P][Ni(i\text{Pr-thiazdt})_2]$ and $[Ph_4P][Ni(c\text{Pr-thiazdt})_2]$. Indeed, for both complexes the interactions within the chains along the *b* axis could be associated with magnetic interactions along this direction. However the temperature dependence of the magnetic susceptibility indicate a Curie-Weiss behavior with θ = +0.7 K for $[Ph_4P][Ni(c\text{Pr-thiazdt})_2]$ and θ = -0.03 K for $[Ph_4P][Ni(i\text{Pr-thiazdt})_2]$ confirming the very weak interactions within the chains and that radical anions are essentially isolated from each other.

Organization of the neutral complexes in the solid state: The neutral complexes $[Ni(R\text{-thiazdt})_2]^0$ (R = iPr, NMe_2), are both organized in uniform stacks. Depending on the substituent on the nitrogen atom, the organization is different, as detailed below. Concerning the *cis*-$[Ni(i\text{Pr-thiazSdt})_2]^0$, within the stacks formed by the complexes with a substituent *i*Pr, there is a longitudinal shift of the molecules relative to each other with the nickel atom of one complex practically above the sulfur atom of the thiazoline ring of the neighboring complex (Figure 6). The distance between planes of molecules is 3.87 Å. The *cis* configuration of the complexes induces the formation of a kind of "insulating sleeve" formed by the *i*Pr substituents: the stacks are separated from each other by the *i*Pr groups, so there is no S•••S contact between stacks.

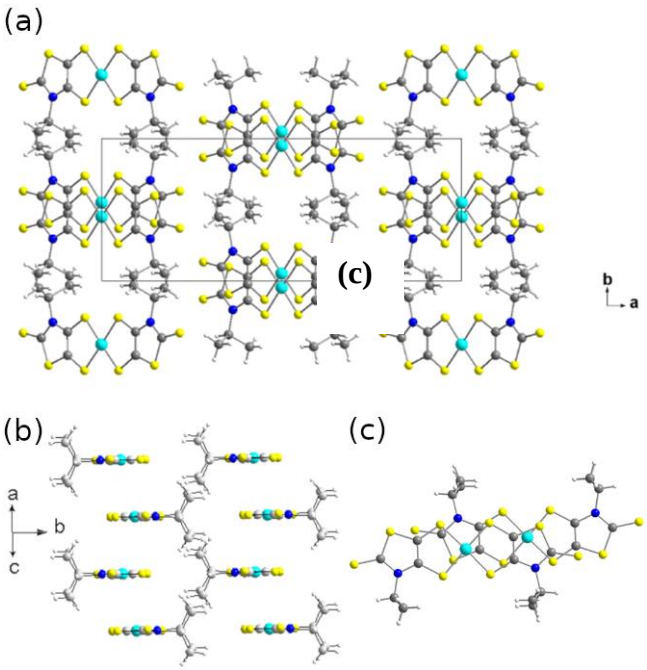

Figure 6. Projection view along *c* axis of the unit cell of $[Ni(iPr\text{-}thiazdt)_2]^0$ (a). View of the organization of the $[Ni(iPr\text{-}thiazdt)_2]^0$ complexes within the stacks (b) and overlap pattern within the stacks (c).

In the case of the neutral nickel complex carrying a NMe_2 group, the molecules are stacked along the *c* axis with a plane-to-plane distance of 3.81 Å (Figure 7). The overlap pattern results from a rotation of the major axis of the molecules and a translation which leads to an overlap with two complexes above and two complexes below as shown in Figure 7. This type of overlap is called spanning overlap. Along the *c* stacking axis, there is no short contact S•••S since the distances are greater than 3.8 Å. On the other hand, along the *b* axis, short S•••S distances of 3.52 and 3.77 Å are observed (Figure 7c). Transport measurements give a low conductivity at room temperature of 2.10^{-6} $S.cm^{-1}$, typical of a semiconductor.

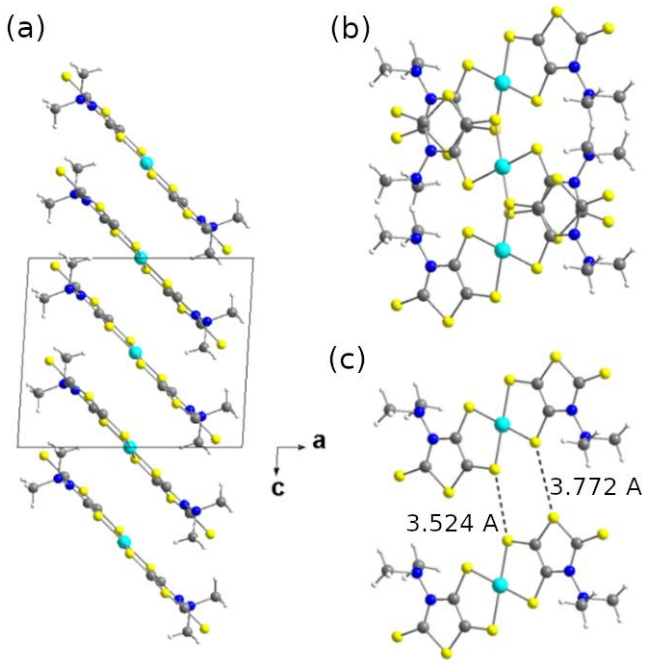

Figure 7. Projection view on the *ac* plane of the unit cell (a), overlap pattern along the *bc* plane (b) and details of the S•••S contacts along *b* (c).

Having in hands the structural characterization of the neutral nickel complexes [Ni(R-thiazdt)$_2$]^0 it was thus of interest to compare the organization of these closed-shell complexes with their gold ones [Au(R-thiazdt)$_2$]$^\bullet$, in order to see the influence of the additional electron of gold complexes on the structural properties. These neutral nickel/gold complexes are not isostructural. An important difference lies in particular in the intermolecular overlap patterns within the stacks (Figure 8). With the substituent *i*Pr, [M(*i*Pr-thiazdt)$_2$], the nickel complex, of cis configuration, gives an almost eclipsed covering with a small lateral offset, while the gold complex of *trans* configuration adopts an original crisscross structure with the gold atoms positioned one above the other The overlaps within the [M(NMe$_2$-thiazdt)$_2$] complexes are also different. For the nickel complex, we also observe a rotation of the long axis of the molecules and a translation, which leads to a spanning overlap. In the case of the gold complex, we find the cross pattern, seen with the isopropyl complex (Figure 8).

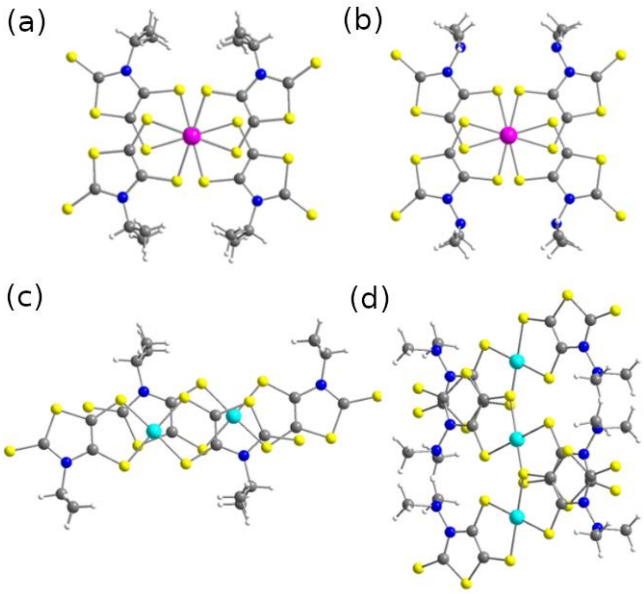

Figure 8. Detail of the overlap patterns between $[M(R\text{-thiazdt})_2]^0$ species with (a) M = Au, R = *i*Pr, (b) M = Au, R = NMe_2, (c) M = Ni, R = *i*Pr and (d) M = Ni, R = NMe_2.

In the case of our neutral complexes $[M(R\text{-thiazdt})_2]^0$ (M = Ni, Au) with bulky or non-bulky substituents, unlike what is observed in the literature, none is isostructural. It can be observed that for the gold complexes the overlaps are optimized, which is not the case for the nickel complexes which present a shifted organization. This type of overlap pattern for the gold complexes is the consequence of a stabilization of the radical species to form chemical bonds by strong antiferromagnetic coupling.

Conclusion

A complete series of bis(dithiolene) monoanionic, and neutral complexes of nickel $[Ni(R\text{-thiazdt})_2]^{-n}$ (n = 1, 0 and R = Pr, *c*Pr, *i*Pr, NMe_2) has been studied. The electrochemical and spectroscopic properties confirm the electron-rich character of the R-thiazdt dithiolate ligand. We have found that the monoanionic nickel complexes $[PPh_4][Ni(R\text{-thiazdt})_2]$ (R = *i*Pr, NMe_2) are isostructural with their gold analogues $[PPh_4][Au(R\text{-thiazdt})_2]$ (R = *i*Pr, NMe_2). On the other hand, despite an organization in uniform stacks, the neutral nickel complexes [Ni(R-

thiazdt)$_2$] (R = *i*Pr, NMe_2) complexes are not isostructural with their gold analogues even with the presence of bulkier substituents. Moreover we isolated one of the rare example of the *cis* isomer in the neutral state, *cis*-[Ni(*i*Pr-thiazdt)$_2$]^0, with this family of ligand while all the other neutral metal bis(dithiolene) complexes were obtained, so far, under the *trans* configuration. Within this study we have shown that with bulky substituents on the dithiolene ligand, the overlap pattern of the closed-shell neutral Ni complexes is different than the one of the open-shell neutral Au complexes.

Experimental Section

All the reactions were performed under an argon atmosphere. Melting points were measured on a Kofler hot-stage apparatus and are uncorrected. Mass spectra were recorded by the Centre Régional de Mesures Physiques de l'Ouest, Rennes. Elemental analyses were performed at Institut de Chimie des Substances Naturelles (CNRS, Gif/Yvette, France). CVs were carried out on a 10^{-3} M solution of complex in CH_2Cl_2 with NBu_4PF_6 0.1 M. Potentials were measured versus Saturated Calomel Electrode (SCE). The spectroelectrochemical setup was performed in CH_2Cl_2 with NBu_4PF_6 0.2 M using a Pt grid as the working electrode, a Pt wire as the counter electrode and SCE reference electrode. Those electrodes are immersed in the electrolyte solution in a typical cuvette electrochemical cell of 1 mm optical path-length, an OTTLE (Optically transparent thin layer electrode). A Shimadzu 3600 spectrophotometer was employed to record the UV-vis-NIR spectra. The electrochemical cell is placed inside the spectrophotometer to measure the absorption of the desired analyte after each gradual oxidation command issued by the potentiostat. Methanol, acetonitrile and dichloromethane were dried using Inert pure solvent column device. Chemicals and materials from commercial sources were

used without further purification. The proligands **1-R** were prepared as previously reported.[23,24]

[PPh_4][Ni(R-thiazdt)$_2$] To a dry two-neck flask containing 1,3-thiazoline-2-thione **1-R** (R =Pr, *i*Pr, *c*Pr, NMe_2: 0.21 g, 0.64 mmol) 7.5 mL of 1M solution of sodium methalonate in MeOH was added under nitrogen atmosphere at room temperature. After stirring for 30 min, a solution containing nickel dichloride ($NiCl_2$) (0.05 g, 0.38 mmol) in 7 mL of dried methanol was added to the reaction mixture followed, 5 h later, by the addition of tetraphenylphosphonium chloride (PPh_4Cl) (0.25 g, 0.64 mmol) in 7 mL of dried methanol. Then the reaction mixture was stirred overnight at room temperature under argon atmosphere. The opaque dark red solution was filtered over a vacuum flask. The resulting solid was washed with MeOH and recrystallized with acetonitrile/toluene solution (1/1) to afford the monoanionic nickel complexes **[PPh_4][Ni(R-thiazdt)$_2$]**.

Formation of the monoanionic complexes from the dianionic one: Under inert atmosphere, [Cp_2Fe][PF_6] (0.03 g, 0.09 mmol) was dissolved in 10 mL of distilled dichloromethane, and the dianionic nickel complex **[PPh_4]$_2$[Ni(R-thiazdt)$_2$]** (0.09 mmol) was added to the reaction medium. After stirring for 1 h, pentane (40 mL) was added and the precipitate was filtered. The monanionic complex **[PPh_4][Ni(R-thiazdt)$_2$]** was recrystallized with a solution of toluene/acetonitrile (1:1) to afford the complex as dark red crystals.

[PPh_4][Ni(Pr-thiazdt)$_2$], $C_{36}H_{34}NiN_2PS_8$; black red crystals. Yield: 0.21 g (74%), mp = 182 °C. UV-vis-NIR (CH_2Cl_2) λ (nm), ε ($M^{-1}.cm^{-1}$): 1282, 17692. HRMS (ESI, Q-Exactive) calcd for $C_{48}H_{48}N_4PS_{16}Ni_2^+$: 1338.78605, found: 1338.7867. Anal. calcd for $C_{36}H_{34}NiN_2PS_8$: C, 51.55; H,3.85; N, 3.34. Found: C, 51.97; H, 3.64; N, 3.22.

[PPh_4][Ni(*i*Pr-thiazdt)$_2$], $C_{36}H_{34}NiN_2PS_8$; black red crystals. Yield: 0.07 g (24%); mp = 206 °C. UV-vis-NIR (CH_2Cl_2) λ (nm), ε ($M^{-1}.cm^{-1}$): 1290 (17400). HRMS (ESI, Q-Exactive) calcd

for $C_{12}H_{14}N_2S_8Ni^-$: 499.82817, found: 499.8283. Anal. calcd for $C_{36}H_{34}NiN_2PS_8$: C, 51.42; H,4.05; N, 3.33. Found: C, 51.36; H, 4.08; N, 3.23.

[PPh$_4$][Ni(*c*Pr-thiazdt)$_2$], $C_{36}H_{30}NiN_2PS_8$; black brown crystals. Yield: 0.17 g (68%), mp = 230 °C. UV-vis-NIR (CH_2Cl_2) λ (nm), ε ($M^{-1}.cm^{-1}$): 1249, 21507. HRMS (ESI, Q-Exactive) calcd for for $C_{48}H_{40}N_4PS_{16}Ni_2^-$: 1330.72345, found: 1330.7228. Anal. calcd for $C_{36}H_{30}NiN_2PS_8$: C, 51.67; H,3.61; N, 3.35. Found: C, 51.18; H, 3.37; N, 3.03.

[PPh$_4$][Ni(NMe$_2$-thiazdt)$_2$], $C_{34}H_{32}NiN_2PS_8$; black brown crystals. Yield: 0.08g (29%); mp = 196 °C. UV-vis-NIR (CH_2Cl_2) λ (nm), ε ($M^{-1}.cm^{-1}$): 1225, 20812. HRMS (ESI, Q-Exactive) calcd for for $C_{44}H_{44}N_8PS_{16}Ni_2^-$: 1342.76705, found: 1342.7680. Anal. calcd for $C_{34}H_{32}NiN_2PS_8$: C, 48.45; H,3.83; N, 6.65. Found: C, 48.30; H, 3.44; N, 6.53.

Electrocrystallizations

In a two compartment cell equipped with Pt electrodes (diameter 1 mm, length 2 cm) $TBAPF_6$ (100 mg, 1 mmol) dissolved in 16 mL of CH_3CN was introduced in both compartment as supporting electrolyte. The monoanionic nickel complex **[PPh$_4$][Ni(R-thiazdt)$_2$]** (8 mg, 0.95 10^{-3} mmol) was introduced in the anodic compartment. The current intensity was adjusted from 0.3 to 0.5 µA, and the reaction was left during 5 days to 5 weeks according to R group. Crystals of the neutral complexes [Ni(*i*Pr-thiazdt)$_2$] and [Ni(NMe$_2$-thiazdt)$_2$] were collected on the anode as black needles. These neutral complexes exhibit a mp > 250 °C.

X-Ray Crystallography

Details of the structural analyses for the four compounds are summarized in Table 3. Data collections were performed on an APEXII Bruker-AXS diffractometer equipped with a CCD camera for [Ph$_4$P][Ni(*i*Pr-thiazdt)$_2$], [Ph$_4$P][Ni(NMe$_2$-thiazdt)$_2$] and [Ni(NMe$_2$-thiazdt)$_2$]^0, and

on D8 VENTURE Bruker AXS diffractometer for $[Ph_4P][Ni(cPr\text{-}thiazdt)_2]$ and $[Ni(iPr\text{-}thiazdt)_2]^0$. Both diffractometers, equipped with graphite-monochromated Mo-Kα radiation (λ = 0.71073 Å), are located at the centre de Diffractométrie (CDFIX), Université de Rennes 1, France. Structures were solved by dual-space algorithm using SHELXT program,[28] and then refined with full-matrix least-squares methods based on F^2 (*SHELXL*).[29] All non-hydrogen atoms were refined with anisotropic atomic displacement parameters. H atoms were finally included in their calculated positions and treating as riding on their parent atom with constrained thermal parameter with exception for the hydrogen atoms of the disordered water molecule in $[Ph_4P][Ni(iPr\text{-}thiazdt)_2]$ that have been fully omitted in the structural model. Crystallographic data have been deposited to the Cambridge Crystallographic Data Center (CCDC number 2173320-2173324). These data are provided free of charge by the joint Cambridge Crystallographic Data Centre and Fachinformationszentrum Karlsruhe Access Structures service www.ccdc.cam.ac.uk/structures.

Table 3 Crystallographic data

	$[Ph_4P][Ni(iPr\text{-}thiazdt)_2]$ $0.44H_2O$	$[Ph_4P][Ni(NMe_2\text{-}thiazdt)_2]$.	$[Ph_4P][Ni(cPr\text{-}thiazdt)_2]$ $2CH_3CN$	$[Ni(iPr\text{-}thiazdt)_2]$	$[Ni(NMe_2\text{-}thiazdt)_2]$
CCDC	2173323	2173322	2173324	2173321	2173320
Formulae	$C_{36}H_{34}N_2NiOPS_8$	$C_{34}H_{32}N_4NiPS_8$	$C_{40}H_{36}N_4NiPS_8$	$C_{10}H_{14}N_2NiS_8$	$C_{10}H_{12}N_4NiS_8$
FW ($g.mol^{-1}$)	847.83	842.79	918.89	501.44	503.43
System	monoclinic	monoclinic	monoclinic	monoclinic	monoclinic
Space group	C2/c	$P2_1/n$	C2/c	C2/c	$P2_1/c$
a (Å)	29.093(10)	10.0387(5)	26.306(6)	21.4589(11)	12.2012(3)
b (Å)	7.227(3)	16.8836(11)	7.1792(16)	8.4051(4)	7.3291(2)
c (Å)	22.320(8)	22.3183(16)	24.751(5)	10.5398(5)	10.3458(2)
α (deg)	90	90	90	90	90
β (deg)	124.883(16)	98.082(2)	115.825(8)	97.079(2)	93.350(1)
γ (deg)	90	90	90	90	90
V ($Å^3$)	3850(2)	3745.1(4)	4207.6(16)	1886.51(16)	923.58(4)
T (K)	150(2)	150(2)	150(2)	150(2)	150(2)
Z	4	4	4	4	2
D_{calc} ($g.cm^{-1}$)	1.463	1.495	1.451	1.766	1.810
μ (mm^{-1})	1.012	1.039	0.931	1.911	1.955
Total refls	12889	32792	15392	7185	9396
Abs corr	multi-scan	multi-scan	multi-scan	multi-scan	multi-scan
Uniq refls	4349	8479	4805	2116	2127
R_{int}	0.0440	0.0823	0.0549	0.0173	0.0322
Uniq refls ($I > 2\sigma(I)$)	3281	6052	4059	2013	1844
R_1	0.0394,0.0796	0.0454, 0.0923	0.0760, 0.1882	0.0203, 0.0503	0.0234, 0.0555
wR_2 (all data)	0.0598, 0.0907	0.0722, 0.1026	0.0899, 0.1961	0.0218, 0.0513	0.0292, 0.0582
GOF	1.081	1.036	1.192	1.097	1.042

Conflicts of interest

There are no conflicts to declare.

Acknowledgements

We thank T Guizouarn for the SQUID measurements.

Keywords: crystal structure, dithiolene ligand, electrochemistry, gold complex, nickel complex

References

[1] B. Garreau-de Bonneval, K. I. Moineau-Chane Ching, F. Alary, T.-T. Bui, L. Valade, *Coord. Chem. Rev*. **2010**, *254*, 1457–1467.

[2] T. Naito, *Inorganics* **2020**, *8*, 53 (1–27).

[3] M. F. G. Velho, R. A. L. Silva, D. Belo, *J. Mater. Chem. C* **2021**, *9*, 10591–10609.

[4] H. Tanaka, Y. Okano, H. Kobayashi, W. Suzuki, A. Kobayashi, *Science* **2001**, *291*, 285–287.

[5] A. Kobayashi, E. Fujiwara, H. Kobayashi, *Chem. Rev.*, **2004**, *104*, 5243–5264.

[6] W. Suzuki, E. Fujiwara, A. Kobayashi, Y. Fujishiro, E. Nishibori, M. Takata, M. Sakata, H. Fujiwara, H. Kobayashi, H. *J. Am. Chem. Soc.* **2003**, *125*, 1486–1487.

[7] O. J. Dautel, M. Fourmigué, E. Canadell, P. Auban-Senzier, *Adv. Funct. Mater*. **2002**, *12*, 693–698.

[8] R. Perochon, C. Poriel, O. Jeannin, L. Piekara-Sady, M. Fourmigué, *Eur. J. Inorg. Chem.* **2009**, 5413–5421

[9] (a) M. Megnamisi-Belombe, B. Nuber, *Bull. Chem. Soc. Jpn*. **1989**, *62*, 4092–4094; (b) Q. Miao, J. Gao, Z. Wang, H. Yu, Y. Luo, T. Ma, *Inorg. Chim. Acta* **2011**, *367*, 619–627.

[10] R. Perochon, L. Piekara-Sady, W. Jurga, R. Clérac, M. Fourmigué, *Dalton Trans.* **2009**, 3052–3061

[11] D. G. Branzea, F. Pop, P. Auban-Senzier, R. Clérac, P. Alemany, E. Canadell, N. Avarvari, *J. Am. Chem. Soc*. **2016**, *138*, 6838–6851.

[12] M. M. Andrade, R. A. L. Silva, I. C. Santos, E. B. Lopes, S. Rabaça, L. C. J. Pereira, J. T. Coutinho, J. P. Telo, C. Rovira, M. Almeida, D. Belo, *Inorg. Chem. Front*. **2017**, *4*, 270–280.

[13] M. Sasa, E. Fujiwara, A. Kobayashi, S. Ishibashi, K. Terakura, Y. Okano, H. Fujiwara, H. Kobayashi, *J. Mater. Chem.* **2005**, *15*, 155–163.

[14] A. Kobayashi, H. Tanaka, M. Kumasaki, H. Torii, B. Narymbetov, T. Adachi, *J. Am. Chem. Soc.* **1999**, *121*, 10763–10771.

[15] B. Zhou, H. Yajima, Y. Idobata, A. Kobayashi, T. Kobayashi, E. Nishibori, H. Sawa, H. Kobayashi, *Chem. Lett.* **2012**, *41*, 154–156.

[16] (a) H. Kim, A. Kobayashi, Y. Sasaki, R. Kato, H. Kobayashi, *Bull. Chem. Soc. Jpn.* **1988**, *61*, 579.

[17] S. S. Nagapeytan, V. E. Shklover, L. V. Vetoshkina, A. I. Kotov, L. Y. Ukhin, Y. T. Struchkov, E. B. Yagubskii, *Mater. Sci.* **1988**, *14*, 5–9.

[18] A. J. Schultz, H. H. Wang, L. C. Soderholm, T. L. Sifter, J. M. Williams, K. Bechgaard, M.-H. Whangbo, *Inorg. Chem*. **1987**, *26*, 3757–3761.

[19] (a) A. Filatre-Furcate, N. Bellec, O. Jeannin, P. Auban-Senzier, M. Fourmigué, A. Vacher, D. Lorcy, *Inorg. Chem.* **2014**, *53*, 8681–8690. (b) H. Hachem, H. Cui, T. Tsumuraya, R. Kato, O. Jeannin, M. Fourmigué, D. Lorcy, *J. Mater. Chem. C* **2020**, *8*, 11581–11592.

[20] (a) N. Tenn, N. Bellec, O. Jeannin, L. Piekara-Sady, P. Auban-Senzier, J. Íñiguez, E. Canadell, D. Lorcy, *J. Am. Chem. Soc*. **2009**, *131*, 16961−16967. (b) Y. Le Gal, T. Roisnel, P. Auban-Senzier, N. Bellec, J. Íñiguez, E. Canadell, D. Lorcy, *J. Am. Chem. Soc.* **2018**, *140*, 6998−7004.

[21] A Filatre-Furcate, P. Auban-Senzier, M. Fourmigué, T. Roisnel, V. Dorcet, D. Lorcy, *Dalton Trans.* **2015**, *44*, 15683–15689. (b) H. Hachem, Z. Xu, N. Bellec, O. Jeannin, P. Auban-Senzier, T. Guizouarn, M. Fourmigué, D. Lorcy, *Dalton Trans.* **2018**, *47*, 6580–6589.

[22] H. Hachem, N. Bellec, M. Fourmigué, D. Lorcy, *Dalton Trans.*, **2020**, *49*, 6056–6064.

[23] A Filatre-Furcate, N. Bellec, O. Jeannin, P. Auban-Senzier, M. Fourmigué, J. Íñiguez, E. Canadell, B. Brière, V. Ta Phuoc, D. Lorcy, *Inorg. Chem*. **2016**, *55*, 6036–6046.

[24] A. Filatre-Furcate, T. Roisnel, M. Fourmigué, O. Jeannin, N. Bellec, P. Auban-Senzier, D. Lorcy, *Chem. Eur. J.* **2017**, *23*, 16004–16013.

[25] (a) A. Sugumori, N. Tachiya, M. Kajitani, T. Akiyama, *Organometallics* **1996**, *15*, 5664–5668.

[26] S. Eid, M. Fourmigué, T. Roisnel, D. Lorcy, *Inorg. Chem.* **2007**, *46*, 10647–10654.

[27] (a) A. H. Maki, N. Edelstein, A. Davison, R. H. Holm, *J. Am. Chem. Soc.* **1964**, *86*, 4580−4587. (b) R. D. Schmidt, A. H. Maki, *J. Am. Chem. Soc.* **1968**, *90*, 2288−2292.

[28] G. M. Sheldrick, *Acta Cryst.* **2015**, *A71*, 3–8.

[29] G. M. Sheldrick, *Acta Cryst.* **2015**, *C71*, 3–8.

For TOC

From a complete series of nickel bis(dithiolene) monoanionic and neutral complexes [Ni(R-thiazdt)$_2$]$^{-n}$ (n = 1, 0 and R = Pr, *c*Pr, *i*Pr, NMe$_2$), we show that monoanionic Ni complexes are isostructural with their gold analogues, while the overlap pattern of the closed-shell neutral Ni complexes is different than the one of the open-shell neutral Au complexes.